THE JOURNAL OF BIOLOGICAL CHEMISTRY VOL. 285, NO. 38, pp. 29179–29190, September 17, 2010

Neobiosynthesis of Glycosphingolipids by Plasma Membrane-associated Glycosyltransferases*[S]

Received for publication, March 14, 2010, and in revised form, June 21, 2010 Published, JBC Papers in Press, July 16, 2010, DOI 10.1074/jbc.M110.123422

Pilar M. Crespo[1,2], **Vanina Torres Demichelis**[1,3], **and José L. Daniotti**[4]

From the Centro de Investigaciones en Química Biológica de Córdoba (CIQUIBIC, UNC-CONICET), Departamento de Química Biológica, Facultad de Ciencias Químicas, Universidad Nacional de Córdoba, Córdoba X5000HUA, Argentina

Gangliosides, complex glycosphingolipids containing sialic acids, are synthesized in the endoplasmic reticulum and in the Golgi complex. These neobiosynthesized gangliosides move via vesicular transport to the plasma membrane, becoming components of the external leaflet. Gangliosides can undergo endocytosis followed by recycling to the cell surface or sorting to the Golgi complex or lysosomes for remodeling and catabolism. Recently, glycosphingolipid catabolic enzymes (glycohydrolases) have been found to be associated with the plasma membrane, where they display activity on the membrane components. In this work, we demonstrated that ecto-ganglioside glycosyltransferases may catalyze ganglioside synthesis outside the Golgi compartment, particularly at the cell surface. Specifically, we report the first direct evidence of expression and activity of CMP-NeuAc: GM3 sialyltransferase (Sial-T2) at the cell surface of epithelial and melanoma cells, with membrane-integrated ecto-Sial-T2 being able to sialylate endogenously synthesized GM3 ganglioside as well as exogenously incorporated substrate. Interestingly, we also showed that ecto-Sial-T2 was able to synthesize GD3 ganglioside at the cell surface using the endogenously synthesized cytidine monophospho-*N*-acetylneuraminic acid (CMP-NeuAc) available at the extracellular milieu. In addition, the expression of UDP-GalNAc:LacCer/GM3/GD3 *N*-acetylgalactosaminyltransferase (GalNAc-T) was also detected at the cell surface of epithelial cells, whose catalytic activity was only observed after feeding the cells with exogenous GM3 substrate. Thus, the relative interplay between the plasma membrane-associated glycosyltransferase and glycohydrolase activities, even when acting on a common substrate, emerges as a potential level of regulation of the local glycosphingolipid composition in response to different external and internal stimuli.

Gangliosides are sialic acid-containing glycosphingolipids that are located mainly at the outer leaflet of the plasma membrane of eukaryotic cells and participate in cell surface events such as the modulation of growth factor receptors and cell-to-cell and cell-to-matrix interactions (1–6). They are synthesized in the lumen of the Golgi cisternae by a complex system of membrane-bound glycolipid acceptors, nucleotide sugar donors, glycosyltransferases, and nucleotide sugar transporters (7, 8). These neosynthesized gangliosides move through the Golgi complex to the plasma membrane via the luminal surface of transport vesicles (9–12). Then, after their arrival at the plasma membrane, the gangliosides can undergo endocytosis, and once internalized, they can be: (i) recycled back to the plasma membrane directly from early or recycling endosomes; (ii) sorted from endosomes to the Golgi complex, where they can be reglycosylated; or (iii) degraded at the lysosomal level (8, 13–15).

It has been assumed that glycosphingolipid synthesis, including gangliosides, is mainly regulated at the transcriptional and post-transcriptional levels of glycolipid glycosyltransferases and specific transport proteins (7, 16). However, an additional level of regulation of glycosphingolipid expression has been recently suggested to occur at the plasma membrane level, with the existence being reported of a plasma membrane-associated sialidase, termed Neu3, which is able to trigger selective ganglioside desialylation in different cell types (17–19). Moreover, β-hexosaminidase (20), β-glucosidase, and β-galactosidase (21) activities have also been demonstrated at the cell surface, suggesting their role in the remodeling of the plasma membrane glycosphingolipids, thus contributing to modulate lipid composition and membrane organization, and consequently, different signaling processes (21, 22).

In this work, we focused our attention on identifying the neobiosynthesis of gangliosides outside the Golgi compartment, particularly at the plasma membrane. By biochemical approaches, combined with fluorescent confocal microscopy and flow cytometric analysis, we report the first direct evidence for the expression and activity of CMP-NeuAc[5]:GM3 sialyl-

* This work was supported in part by Grants from Secretaría de Ciencia y Tecnología (SECyT)-Universidad Nacional de Córdoba (UNC), Consejo Nacional de Investigaciones Científicas y Técnicas (CONICET), Agencia Nacional de Promoción Científica y Tecnológica (ANPCyT), and Ministerio de Ciencia y Tecnología de la Provincia de Córdoba, Argentina.

[S] The on-line version of this article (available at http://www.jbc.org) contains supplemental Figs. S1–S3.

[1] Both authors contributed equally to this work.

[2] Recipient of CONICET (Argentina) Fellowships.

[3] Recipient of ANPCyT Fellowships.

[4] Career investigator of CONICET (Argentina). To whom correspondence should be addressed: Facultad de Ciencias Químicas, Haya de la Torre y Medina Allende, Ciudad Universitaria, UNC, X5000HUA, Córdoba, Argentina. Tel.: 54-351-4334168/4171; Fax: 54-351-4334074; E-mail: daniotti@dqb.fcq.unc.edu.ar.

[5] The abbreviations used are: CMP-NeuAc, cytidine monophospho-*N*-acetylneuraminic acid; Endo-H, endoglycosidase H; GalNAc-T, UDP-GalNAc:LacCer/GM3/GD3 *N*-acetylgalactosaminyltransferase; Gal-T2, UDP-Gal:GA2/GM2/GD2 galactosyltransferase; HPTLC, high pressure thin layer chromatography; NANase, neuraminidase; P4, D,L-threo-1-fenyl-2-hexadecanoilamino-3-pirrolidino-1-propanol-HCl; Sial-T2, CMP-NeuAc:GM3 sialyltransferase; GM3, NeuAcα2,3Galβ1,4Glc-ceramide; GD3, NeuAcα2,8NeuAcα2,3Galβ1,4Glc-ceramide; GT3, NeuAcα2,8NeuAcα2,8NeuAcα2,3Galβ1,4Glc-ceramide; GM2, GalNacβ1,4(NeuAcα2,3)Galβ1,4Glc-ceramide; GM1, Galβ1,3GalNAcβ1,4-(NeuAcα2,3)-Galβ1,4Glc-ceramide; GD1a, NeuAcα2,3Galβ1,3GalNAcβ1,4-(NeuAcα2,3)Galβ1,4Glc-ceramide; GD2, GalNAcβ1,4(NeuAcα2,8NeuAcα2,3)-Galβ1,4Glc-ceramide.

transferase (Sial-T2; GD3 synthase) at the cell surface of Chinese hamster ovary (CHO)-K1 cells and SK-Mel-28 human melanoma cells. It was demonstrated that membrane-integrated ecto-Sial-T2 was able to sialylate endogenously synthesized GM3 as well as exogenously incorporated substrate. More interestingly, it was also shown that ecto-Sial-T2 was able to synthesize GD3 at the cell surface using the endogenously synthesized CMP-NeuAc available at the extracellular milieu. Additionally, the expression of UDP-GalNAc:LacCer/GM3/GD3 *N*-acetylgalactosaminyltransferase (GalNAc-T) was also detected at the cell surface of CHO-K1 cells, whose catalytic activity was only observed after feeding the cells with exogenous GM3 substrate.

Taken together, our findings provide strong evidence that ecto-ganglioside glycosyltransferases may catalyze ganglioside synthesis outside the Golgi compartment, particularly at the cell surface, which might contribute, together with the glycolipid-catabolizing enzymes, to the local regulation of the plasma membrane glycosphingolipid composition.

EXPERIMENTAL PROCEDURES

Cell Lines, Cell Culture, and DNA Transfection—CHO-K1 cell clones expressing different ganglioside glycosyltransferases had previously been obtained in our laboratory. The following cells were used: wild-type CHO-K1 (CHO-K1^{WT}) cells (American Type Culture Collection (ATCC), Manassas, VA); clone 2, a stable chick Sial-T2 (tagged at the C terminus with the YPYDVPDYA nanopeptide epitope of the viral hemagglutinin (HA)) transfectant expressing the gangliosides GD3 and GT3 (6, 23); clone 3, a stable GalNAc-T (tagged at the C terminus with 10 amino acids of human c-Myc) transfectant mostly expressing gangliosides GM3, GM2, and to a lesser extent GM1 and GD1a (24); clone 4, a stable double transfectant expressing GalNAc-T and UDP-Gal:GA2/GM2/GD2 galactosyltransferase (Gal-T2) tagged at the C terminus with the HA epitope (25, 26) and having an increased expression of GM1 and GD1a; a CHO-K1 clone stably transfected with a plasmid coding for the N terminus of Sial-T2 (amino acids 1–57 containing the cytosolic and transmembrane regions) fused to the N terminus of YFP (Sial-T2-NTD-YFP)[6]; SK-Mel 28 human melanoma cell line (ATCC); and B16 mouse melanoma cell line stably expressing Sial-T2. Cells were grown and maintained at 37 °C in 5% CO_2 in Dulbecco's modified Eagle's medium (DMEM) supplemented with 10% fetal bovine serum (FBS) and antibiotics. Where indicated, cells were transfected with a 1-μg/35-mm dish of the Sial-T2-NTD-YFP plasmid using cationic liposomes (Lipofectamine; Invitrogen) according to the manufacturer's instructions and incubated for 24 h at 37 °C with the transfection reagent and DNA mixture.

Determination of Ganglioside Glycosyltransferase Activities at the Cell Surface—To investigate ganglioside glycosyltransferase activities at the cell surface of the CHO-K1 cell, we developed an intact cell radiolabeling assay by incubating intact cells grown on coverslips in a medium containing different labeled sugar nucleotides. CHO-K1^{WT} cells were fed with 100 μM GM1 for 2 h, and cells from clone 2 and clone 4 were incubated at 37 °C for 2 h in an incubation system containing 20 mM $MnCl_2$, 1 mM $MgCl_2$, 100 mM sodium cacodylate-HCl buffer (pH 6.5 for sialyltransferase activity or pH 7.2 for galactosyl and *N*-acetylgalactosaminyltransferase activities), 100 μM CMP-[^{14}C]NeuAc (for assays using CHO-K1^{WT} and clone 2 cells), or 100 μM UDP-[^{3}H]Gal or 100 μM UDP-[^{3}H]GalNAc (for assays using clone 4 cells with or without 100 μM GM3 feeding for 2 h) in a volume of 30 μl of DMEM. The radiolabeled sugar nucleotide was added at the necessary quantity to reach a specific activity of 166.7 cpm/pmol for CMP-[^{14}C]NeuAc or 1,000 cpm/pmol for UDP-[^{3}H]Gal and UDP-[^{3}H]GalNAc. After incubation, cells were washed with phosphate-buffered saline (PBS), and lipids were extracted with chloroform:methanol (2:1, v/v) and freed from water-soluble contaminants by being passed through a Sephadex G-25 column. The lipid extract was used for radioactivity quantification or for thin-layer chromatography (TLC) analysis, supplemented with the appropriate amounts of standard gangliosides, and chromatographed on high performance TLC plates (HPTLC; Merck) using C:M:0.2% $CaCl_2$ (60:36:8 v/v) as solvent. Standard gangliosides were visualized by exposure of the plate to iodine vapors. Radioactive gangliosides were visualized using a Fuji Photo Film Bio Imagen analyzer or visualized by fluorography after dipping the plate in 0.4% melted 2,5-diphenyloxazole in 2-methylnaphthalene and exposing it to a radiographic film at −70 °C, usually for 15 days (6).

To detect ecto-Sial-T2 activity by immunodetection of the synthesized GD3 using the specific mouse monoclonal antibody anti-GD3 (IgG3) clone R24 (ATCC no. HB-8445), cells from clone 2 (CHO-K1$^{Sial\text{-}T2+}$) or SK-Mel 28 were grown on coverslips and treated for 4 days with 2.4 μM or 1.8 μM, respectively, P4 (Matreya, Pleasant Gap, PA) to reduce GM3, GD3, and the neutral glycolipid content (25). Then, cells were incubated for 3 h with 100 μM GM3 (purified from dog erythrocytes). Where indicated, cells were also incubated for 1 h at 37 °C with 5 mM NaN_3 and 50 mM 2-deoxy-D-glucose for ATP depletion (27). Later, cells were washed repeatedly with 0.2% BSA in PBS to remove the GM3 and then incubated for 2 h in an incubation system containing 20 mM $MnCl_2$, 1 mM $MgCl_2$, 100 mM sodium cacodylate-HCl buffer, pH 6.5, and 100 μM CMP-NeuAc in a volume of 30 μl of DMEM. Finally, coverslips were processed for immunocytochemistry and confocal microscopy analysis.

Internalization Assays—Cells from clone 2 were incubated on ice for 20 min to inhibit intracellular transport. Then, these cells were incubated on ice for 45 min with mouse monoclonal antibody to HA (Sigma-Aldrich) diluted at 1:100. Afterward, cells were washed three times with cold PBS, transferred to 37 °C with fresh prewarmed complete DMEM to allow antibody internalization for different times, and finally washed three times with PBS and fixed for fluorescence microscopy. For transferrin internalization, cells were first incubated for 90 min in DMEM without FBS before being incubated at 4 °C in cold DMEM containing 10 μg/ml Alexa Fluor 647-transferrin (Molecular Probes) and antibody to HA for 45 min. Then, cells were transferred to 37 °C with prewarmed DMEM, without fetal bovine serum but supplemented with 10 μg/ml Alexa Fluor 647-transferrin and processed at different times. Where

[6] W. Spessot, P. M. Crespo, J. L. Daniotti, and H. J. F. Maccioni, Annual Meetings (2007 and 2008) of the Argentine Society for Research in Biochemistry and Molecular Biology (SAIB).

indicated, the noninternalized antibody remaining at the cell surface was removed by acid stripping with 0.5% acetic acid buffer, pH 3.0, containing 0.5 M NaCl for 1 min on ice.

Confocal Immunofluorescence Microscopy—In some experiments, cells grown on coverslips were washed two times with PBS, incubated at 4 °C with the primary antibody for 1 h, fixed with 4% paraformaldehyde in PBS for 20 min at room temperature, and then exposed to the secondary antibody for 90 min at 37 °C. In other experiments, cells on coverslips were fixed with 4% paraformaldehyde in PBS for 20 min at room temperature, permeabilized using 0.1% w/v Triton X-100 in 200 mM glycine for 10 min at 4 °C, incubated in 3% BSA/PBS for 1 h at 37 °C to block the sites of unspecific union, and then exposed to primary and secondary antibodies. After final washes with 1% BSA in PBS, cells were mounted in FluorSave reagent (Calbiochem).

The antibodies used in this study included mouse monoclonal antibody anti-GD3 (R24) diluted 1:100, mouse anti-GFP (Roche Applied Sciences) diluted 1:100, mouse antibody to HA diluted 1:50, and rabbit antibody to c-Myc diluted 1:400. Secondary antibodies used were goat antibody to mouse IgG-Alexa Fluor 488 or goat antibody to rabbit IgG-Alexa Fluor 488 diluted 1:1,000 (Santa Cruz Biotechnology, Santa Cruz, CA).

Confocal images were collected using a Carl Zeiss LSM5 Pascal laser scanning confocal microscope (Carl Zeiss AG) or an Olympus FluoView FV1000 confocal microscope (Olympus Latin America, Miami, FL) equipped with an argon/helium/neon laser and a 100 × (numerical aperture = 1.4) oil immersion objective (Zeiss Plan-Apochromat). Single confocal sections of 0.7 μm were taken parallel to the coverslip (*xy* sections). Final images were compiled with Adobe Photoshop 7.0.

Assessment of Ecto-Sial-T2 Activity by Flow Cytometry—Cells from clone 2 (CHO-K1$^{Sial\text{-}T2+}$) or SK-Mel-28 were seeded in 12-well plates and grown for 5 days with 2.4 μM or 1.8 μM, respectively, P4 to reduce the glycolipid content. Then, cells were incubated for 3 h with 100 μM GM3 and washed repeatedly with 0.2% BSA in PBS to remove the excess GM3. This was followed by incubation for 2 h in a system containing 20 mM $MnCl_2$, 1 mM $MgCl_2$, 100 mM sodium cacodylate-HCl buffer (pH 6.5) and 100 μM CMP-NeuAc in a volume of 300 μl of DMEM, trypsinized, incubated at 4 °C with mouse monoclonal antibody to GD3 (R24, dilution 1:40) for 30 min. Finally, cells were fixed with 4% paraformaldehyde in PBS for 20 min at room temperature before being exposed to the secondary antibody (goat antibody to IgG-Alexa Fluor 488, dilution 1:300) for 30 min at 4 °C. Labeled cells were washed with PBS and resuspended in 200 μl of PBS for fluorescence analysis using a FACSCantoII cytometer (BD Biosciences) equipped with standard optics. For each cell, forward light scatter, orthogonal light scatter, and Alexa Fluor 488 fluorescence were evaluated using BD FACSDiva software (BD Biosciences). A gate was applied in the forward light scatter–orthogonal light scatter dot plot to restrict the analysis to unbroken cells. For the gated cells, the histograms of fluorescence were evaluated.

Immunoprecipitation and Glycosidase Digestions—To immunoprecipitate total Sial-T2 from clone 2, cells were lysed for 60 min on ice with lysis buffer (50 mM Tris-HCl, pH 7.4, 1% w/v Triton X-100, 150 mM NaCl, 3 mg/ml leupeptin, 1 mM phenylmethylsulfonyl fluoride, 3 mg/ml aprotinin, 1 mM EDTA, 0.05% w/v sodium azide), centrifuged for 2 min at 400 × *g*, and the postnuclear supernatant was preabsorbed with protein A-Sepharose beads (GE Healthcare) for 30 min at 4 °C. The cleared lysates were incubated for 2 h on a rotating wheel at 4 °C with protein A-Sepharose beads and monoclonal mouse antibody to HA (1:40). Then, beads were pelleted by centrifugation at 2,500 × *g* for 10 s, washed five times at 4 °C with lysis buffer, washed three times with PBS, and resuspended in 50 μl of PBS.

To immunoprecipitate the plasma membrane-associated Sial-T2, intact cells in suspension were incubated with monoclonal mouse antibody to HA diluted 1:40 for 45 min at room temperature. Then, cells were washed and lysed for 60 min on ice with lysis buffer, and lysates were absorbed with protein A-Sepharose beads for 2 h on a rotating wheel at 4 °C. Beads were pelleted by centrifugation at 2,500 × *g* for 10 s to recuperate the plasma membrane-associated Sial-T2, and the supernatant, containing the intracellular fraction of Sial-T2, was subjected to a second cycle of immunoprecipitation with protein A-Sepharose beads and monoclonal mouse antibody to HA (1:40).

For digestion with neuraminidase (NANase), the immunoprecipitates were incubated in the presence or absence of 300 milliunits/ml NANase from *Vibrio cholerae* for 15 h at 37 °C in 50 mM acetate buffer, pH 5.5. For digestion with endoglycosidase H (Endo-H), immunoprecipitates were incubated in the presence or absence of 350 milliunits/ml Endo-H in 100 mM citrate buffer, pH 5.6, and SDS (0.2% w/v) for 18 h at 37 °C. The incubates were cooled in ice, and the beads were washed with PBS prior to Western blot analysis.

Electrophoresis and Immunoblotting—CHO-K1 cell homogenates and immunoprecipitates were resolved by electrophoresis through 10% SDS-polyacrylamide gels under reducing and nonreducing conditions. Proteins were electrophoretically transferred to nitrocellulose membranes for 90 min at 300 mA, and the protein bands in the nitrocellulose membranes were visualized by Ponceau S staining. For immunoblotting, nonspecific binding sites on the nitrocellulose membrane were blocked with 5% defatted dry milk in 400 mM NaCl, 100 mM Tris-HCl, pH 7.5. A rabbit antibody to HA was used at a dilution of 1:5,000. The antibody to HA was detected by using near-infrared fluorescence (LI-COR Biotechnology, Lincoln, NE) with goat antibody to rabbit IgG coupled to IRDye800CW (LI-COR Biotechnology). Molecular mass was calculated based on calibrated standards (BenchMark prestained protein ladder; Invitrogen) run in every gel. The relative contribution of individual bands was calculated using the computer software Odyssey Application Software version 2.1 (LI-COR Odyssey). Final images were compiled with Adobe Photoshop 7.0.

Biotinylation and Streptavidin Precipitation—Exposed ecto-Sial-T2 on intact cell monolayers was biotinylated using EZ-link Sulfo-NHS-SS Biotin (Pierce) and isolated using streptavidin-agarose beads (Sigma-Aldrich). CHO-K1$^{Sial\text{-}T2+}$ cells were placed on ice and washed three times with PBS. Then, cells were then incubated with EZ-link Sulfo-NHS-SS-Biotin at a final concentration of 0.5 mg/ml into PBS for 60 min at 4 °C, followed by glycine (100 mM) in PBS to quench unbound labeling reagent, before being washed two times with PBS to completely remove any remaining quenching buffer. Biotinylated cells

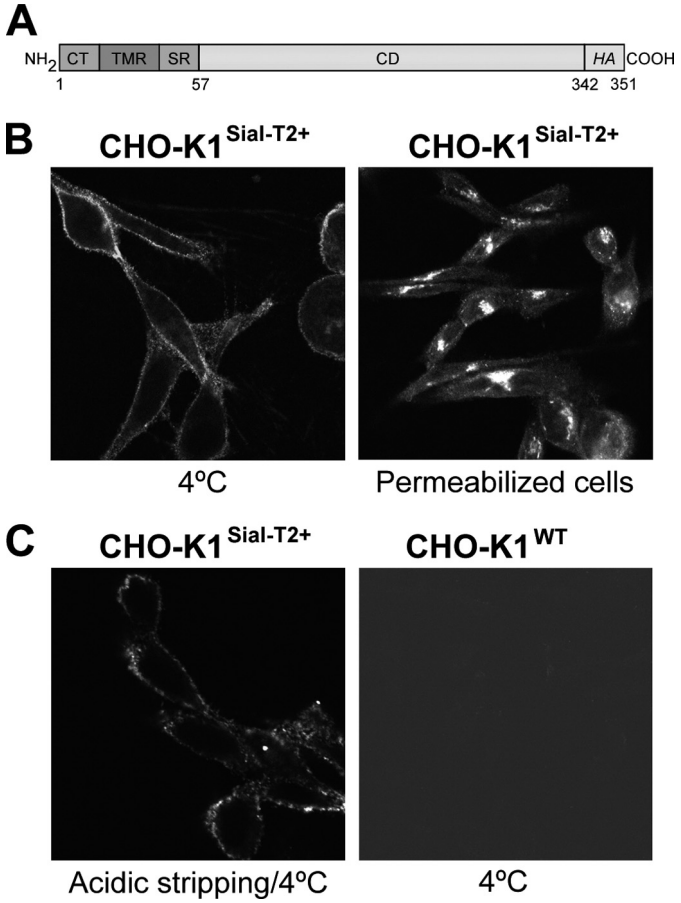

FIGURE 1. **Immunofluorescence detection of Sial-T2 in CHO-K1 cells.** *A*, schematic representation of the Sial-T2-HA construct used to generate clone 2 (CHO-K1$^{Sial\text{-}T2+}$) is shown. *CT*, cytoplasmic tail; *TMR*, transmembrane region; *SR*, stem region; *CD*, catalytic domain; and *HA*, nanopeptide epitope of the viral hemagglutinin. *B*, Sial-T2-HA-expressing CHO-K1 cells (CHO-K1$^{Sial\text{-}T2+}$) were immunostained with an antibody to HA at 4 °C for 45 min and then fixed and incubated with a secondary antibody conjugated to Alexa Fluor 488 (4 °C, *left panel*). Alternatively, CHO-K1$^{Sial\text{-}T2+}$ cells were fixed and permeabilized before immunostaining with antibody to HA and secondary antibody conjugated to Alexa Fluor 488 (Permeabilized cells, *right panel*). *C*, CHO-K1$^{Sial\text{-}T2+}$ cells were incubated with acetate buffer at 4 °C for 1 min before immunostaining with antibody to HA and secondary antibody conjugated to Alexa Fluor 488 (Acidic stripping/4 °C, *left panel*). Wild-type CHO-K1 cells (CHO-K1^{WT}) were incubated at 4 °C with antibody to HA at 4 °C for 60 min and then fixed and incubated with secondary antibody conjugated to Alexa Fluor 488 (4 °C, *right panel*). The image contrast in CHO-K1^{WT} cells was reduced to show the presence of cells. Single confocal sections were taken every 0.7 μm parallel to the coverslip.

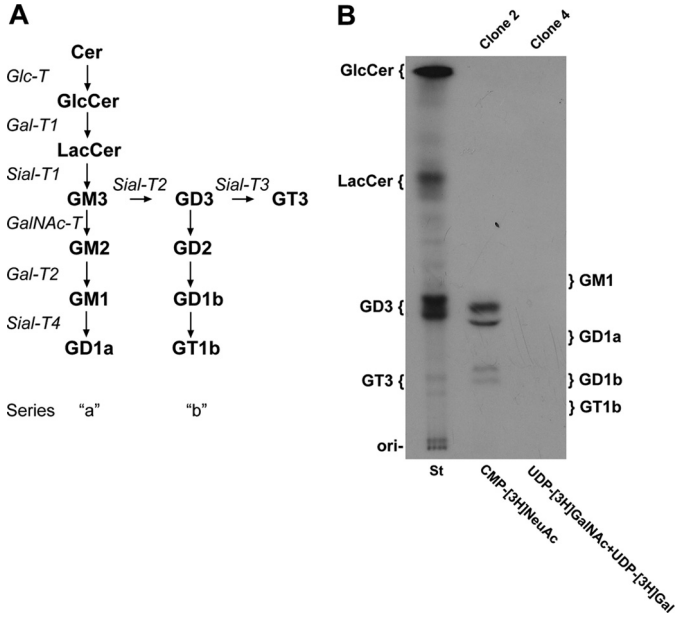

FIGURE 2. **Ganglioside glycosyltransferase activities at the cell surface of CHO-K1 cells.** *A*, schematic representation of the pathway of glycolipid biosynthesis is shown. *Cer*, ceramide; *GlcCer*, glucosylceramide; *LacCer*, lactosylceramide. *B*, CHO-K1$^{Sial\text{-}T2+}$ (clone 2) or CHO-K1$^{GalNAc\text{-}T+/Gal\text{-}T2+}$ (clone 4) cells were incubated for 2 h with CMP-[^{14}C]NeuAc, or UDP-[^{3}H]GalNAc and UDP-[^{3}H]Gal, respectively. Next, lipid extracts were purified, resolved by HPTLC, and visualized as indicated under "Experimental Procedures." The positions of co-chromatographed radioactive glycolipid standards (*St*) are indicated on the *left* of the *plate*. GM1, GD1a, GD1b, and GT1b were also co-chromatographed and visualized by exposing the plate to iodine vapor (ganglioside positions are indicated on the *right* of the *plate*). Lipids migrate as multiple bands on the HPTLC plate because of the heterogeneity of the fatty acyl chains of the molecules.

were scraped off the plates in lysis buffer (20 mM Tris-HCl, pH 7.5, 1 mM EDTA, 1% w/v Triton X-100, 150 mM NaCl, 10 mM glycine, 3 mg/ml leupeptin, 1 mM phenylmethylsulfonyl fluoride, 3 mg/ml aprotinin) and agitated on a shaker for 60 min at 4 °C. The cell lysate was centrifuged for 10 min at 14,000 × *g*, and the resulting supernatant was incubated with prewashed streptavidin-agarose beads, suspended in lysis buffer, and mixed at 4 °C for 3 h. The beads were recovered by centrifugation (5,000 × *g* for 15 s) and then washed three times in lysis buffer without Triton X-100. The resulting biotinylated cell surface proteins were resolved by SDS-PAGE gel, transferred onto a membrane, and probed with antibody to HA to detect the presence of Sial-T2 as mentioned above under "Electrophoresis and Immunoblotting."

RESULTS

Sial-T2 Is Expressed at the Plasma Membrane of CHO-K1 Cells—The presence of Sial-T2 was previously demonstrated in the medial-trans cisternae of the Golgi complex (23), where it synthesizes the gangliosides GD3 and GT3. Using confocal immunofluorescence microscopy, we attempted to detect the presence of Sial-T2 at the plasma membrane (ecto-Sial-T2) of CHO-K1 cells stably expressing a HA-tagged version of the enzyme (clone 2) (Fig. 1*A*). Briefly, Sial-T2 expressing CHO-K1 (CHO-K1$^{Sial\text{-}T2+}$) and CHO-K1^{WT} cells were first incubated at 4 °C to inhibit intracellular transport and then with antibody to HA at 4 °C for 45 min to allow membrane binding. Next, cells were fixed and processed for immunofluorescence. Sial-T2 was found to decorate the cell surface of CHO-K1$^{Sial\text{-}T2+}$, whereas in permeabilized cells Sial-T2 showed the typical perinuclear localization characteristic of the Golgi complex (Fig. 1*B*). For the control, we observed that CHO-K1^{WT} did not bind antibody to HA (Fig. 1*C*). In addition, a possible association to the plasma membrane of secreted and soluble Sial-T2 (23) was ruled out by acidic stripping before HA immunodetection (Fig. 1*C*). Interestingly, ecto-Sial-T2 was also detected in B16 mouse melanoma cells, but which stably expressed 10-fold less Sial-T2 than CHO-K1$^{Sial\text{-}T2+}$ cells (results not shown). In addition, cell surface GD3 synthesis was also detected in SK-Mel-28 human melanoma cells endogenously expressing Sial-T2 (see Fig. 5). Thus, these results revealed the presence of membrane-inte-

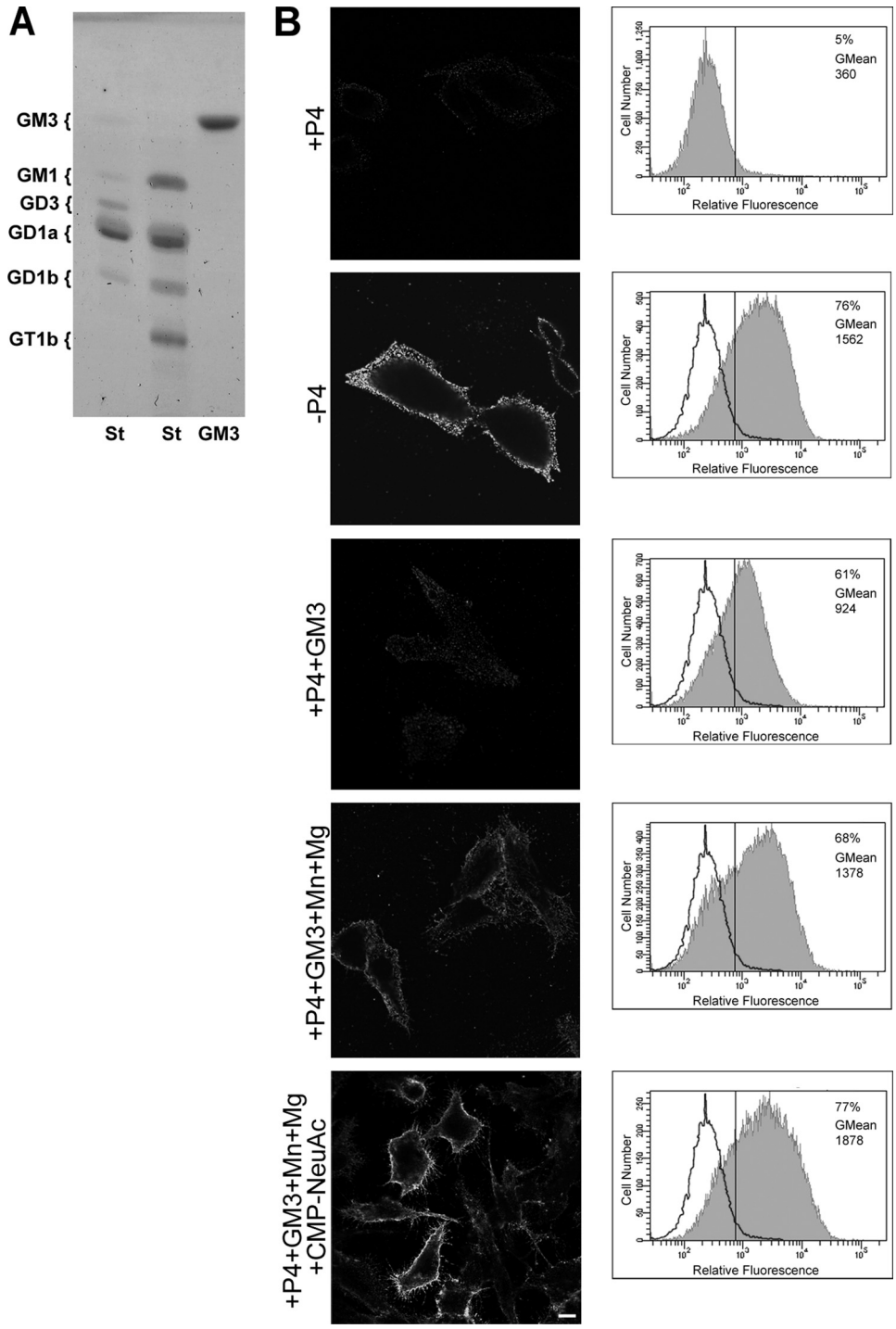

FIGURE 3. **Ecto-Sial-T2 sialylates exogenously incorporated GM3 in CHO-K1$^{Sial\text{-}T2+}$ cells.** *A*, chromatographic analysis of GM3 ganglioside used in the experiments in *B* is shown. GM3 and standard (*St*) glycolipids were co-chromatographed on HPTLC and revealed by orcinol staining. The positions of glycolipid standards are indicated on the *left*. *B*, CHO-K1$^{Sial\text{-}T2+}$ cells were grown with P4 (+*P4*; *first* and *third* to *fifth rows*) or without P4 (−*P4*, *second row*) for 4 days. Then, cells were treated with 100 μM GM3, washed, and incubated at 37 °C for 2 h in a medium containing only DMEM (+*P4*+*GM3*, *third row*) or in a medium containing Mn^{2+} and Mg^{2+} (+*P4*+*GM3*+*Mn*+*Mg*, *fourth row*) or CMP-NeuAc, Mn^{2+} and Mg^{2+} (+*P4*+*GM3*+*Mn*+*Mg*+*CMP-NeuAc*, *fifth row*). P4 inhibitor remained present throughout the experiments. *Left panels*, cells were washed, immunostained with antibody to GD3 (R24) at 4 °C for 60 min, and then fixed and incubated with secondary antibody conjugated to Alexa Fluor 488. Single confocal sections were taken every 0.7 μm parallel to the coverslip. *Right panels*, cells were trypsinized, incubated at 4 °C with R24 antibody for 30 min, and then fixed and exposed to the secondary antibody for 30 min at 4 °C. Labeled cells were washed, resuspended in 200 μl of PBS, and fluorescence-quantified using flow cytometric analysis. The *vertical line* in each histogram marks the upper limit of control (+P4) to assess frequencies (%) of positive cells. The geometric mean fluorescence intensity (*GMean*) is also indicated. *Scale bar*, 10 μm.

grated ecto-Sial-T2 on plasma membrane, suggesting that glycolipid sialylation might occur outside the Golgi complex.

Plasma Membrane-associated Sial-T2 Is Able to Sialylate Endogenously Expressed GM3—To investigate ganglioside glycosyltransferase activities (see *scheme* in Fig. 2*A*) on the cell surface of the CHO-K1 cell, we developed an intact cell radiolabeling assay by incubating the cells in a medium containing different labeled nucleotide sugars. Thus, CHO-K1$^{Sial\text{-}T2+}$ cells were incubated with CMP-[^{14}C]NeuAc for 2 h and the radioactive glycolipids purified and revealed by HPTLC. As shown in Fig. 2*B*, CHO-K1$^{Sial\text{-}T2+}$ cells were able to synthesize GD3 and, to a lesser extent, GT3. On the other hand, when CHO-K1 cells, genetically modified to express gangliosides from the "a" series (GM2, GM1, and GD1a; see Fig. 2*A*) by stable expression of GalNAc-T and Gal-T2 (clone 4), were incubated with UDP-[^{3}H]GalNAc (to label GM2) and UDP-[^{3}H]Gal (to label GM1), synthesis of the complex glycolipid could not be observed (Fig. 2*B*). In addition, CHO-K1^{WT} cells (which only express GM3) (26) and cells from clone 4 incubated with CMP-[^{14}C]NeuAc were not able to synthesize GM3 and GD1a, respectively, discarding any activity of Sial-T1 or Sial-T4 at the cell surface of these cell lines (results not shown). The absence of GM3 and GD1a syntheses and the nonappreciable uptake of CMP-[^{14}C]NeuAc preclude the possibility that the nucleotide sugar is transported from the extracellular milieu to the Golgi complex for further glycolipid synthesis.

Cell Surface-located Sial-T2 Sialylates Exogenously Incorporated GM3—To develop a more versatile, safer, cheaper and less time-consuming assay to measure ecto-Sial-T2 activity under different experimental conditions, CHO-K1$^{Sial\text{-}T2+}$ cells were treated with P4, a potent inhibitor of ceramide glucosyltransferase, for 4 days to

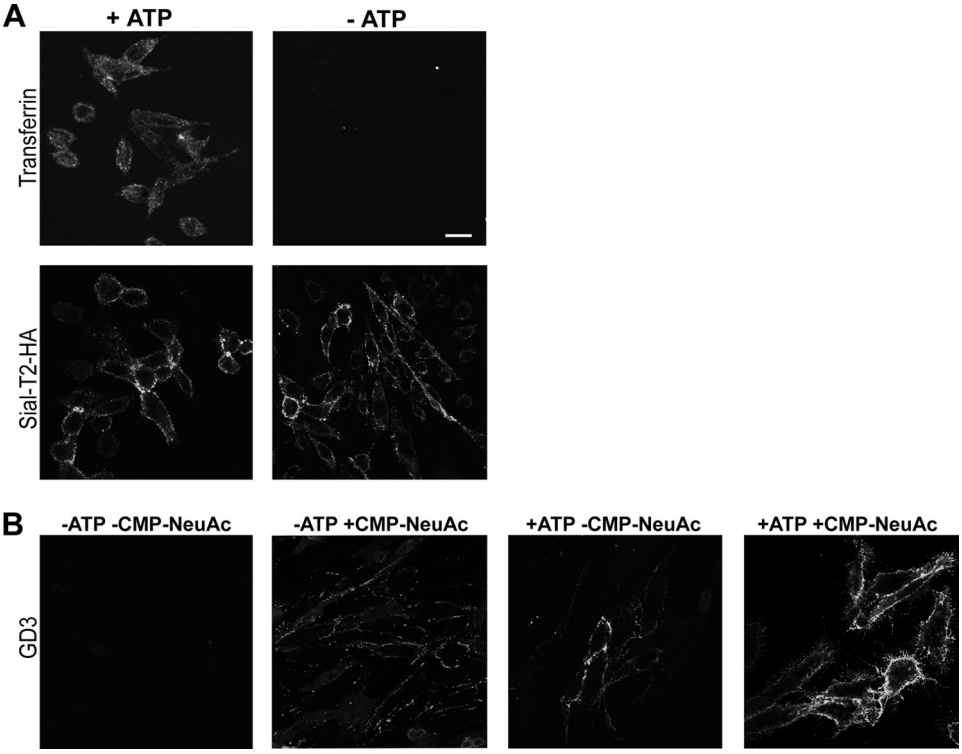

FIGURE 4. **Inhibition of vesicular transport reduces GD3 synthesis at the cell surface of CHO-K1$^{Sial\text{-}T2+}$ cells.** *A*, CHO-K1$^{Sial\text{-}T2+}$ cells were incubated for 1 h in PBS containing 50 mM 2-deoxyglucose and 5 mM NaN_3 (*−ATP*) or complete DMEM (*+ATP*). Cells were labeled with Alexa Fluor 647-transferrin and then fixed and visualized by confocal microscopy (*upper panels*). Alternatively, cells were immunostained with antibody to HA at 4 °C for 1 h (Sial-T2-HA) and then fixed and incubated with secondary antibody conjugated to Alexa Fluor 488. Single confocal sections of 0.7 μm were taken parallel to the coverslip. *B*, CHO-K1$^{Sial\text{-}T2+}$ cells were treated with P4 for 4 days and incubated for 3 h with 100 μM GM3. Then, cells were incubated for 1 h in PBS containing 5 mM NaN_3 and 50 mM 2-deoxy-D-glucose (*−ATP*), or complete DMEM (*+ATP*). Finally, cells were incubated for 2 h at 37 °C in a medium containing P4, Mn^{2+}, and Mg^{2+}, both in the presence (*+CMP-NeuAc*, *second* and *fourth panels*) or in the absence of CMP-NeuAc (*−CMP-NeuAc*, *first* and *third panels*). Then, cells were washed and immunostained with R24 antibody to GD3. Single confocal sections were taken every 0.7 μm parallel to the coverslip. *Scale bar*, 10 μm.

reduce GM3, GD3, and neutral glycolipid content (Fig. 3*B*, see *+P4*). Then, cells were incubated for 2 h with 100 μM GM3 before being washed and incubated in a medium containing CMP-NeuAc, Mn^{2+} and Mg^{2+} at 37 °C for 2 h in the presence of P4 inhibitor, with the Sial-T2 activity being determined by immunodetection of the synthesized GD3 using the specific monoclonal antibody R24. As shown in Fig. 3*B* (*fifth row*), GD3 was detected at the cell surface of P4-treated CHO-K1$^{Sial\text{-}T2+}$ cells, indicating that Sial-T2 was able to use the exogenously incorporated acceptor (GM3) to catalytically convert it to disialoganglioside (GD3) by the addition of one molecule of sialic acid. In contrast, although a reduced amount of GD3 synthesis was observed when P4-treated CHO-K1$^{Sial\text{-}T2+}$ cells were fed with GM3 and incubated only in DMEM (culture medium containing 0.814 mM Mg^{2+}) (Fig. 3*B*, *third row*), a significant increase of GD3 synthesis was observed when P4-treated CHO-K1$^{Sial\text{-}T2+}$ cells were fed with exogenous GM3 and incubated in a medium containing bivalent cations (1 mM Mn^{2+} and 20 mM Mg^{2+}) in the absence of exogenous CMP-NeuAc (Fig. 3*B*, *fourth row*). Thus, these results strongly suggest that CHO-K1 cells supplied endogenously synthesized CMP-NeuAc to synthesize GD3 at the cell surface and that the exogenous administration of the sugar nucleotide donor significantly increased the synthesis of the disialoganglioside. Ecto-Sial-T2 activity was also investigated by flow cytometric assays (Fig. 3*B*, *right panels*). The Sial-T2 activity values at the cell surface of CHO-K1$^{Sial\text{-}T2+}$ cells were very low in P4-treated cells, but a noticeable increase in the fluorescent intensity was observed for the other analyzed experimental conditions (GM3 plus cations, and GM3 plus cations and exogenous CMP-NeuAc) in agreement with results obtained by confocal immunofluorescent analysis (Fig. 3*B*, *left panels*). Therefore, under these experimental conditions, we discard GD3 synthesis occurring in intracellular endosomal compartments because it was observed that ecto-Sial-T2-HA did not appreciably internalize and recycle over a period of 2 h, when analyzed by an antibody-binding technique (results not shown). In addition, the reduced amount of GD3 synthesis in P4-treated cells fed with 100 μM GM3 and incubated only in DMEM (Fig. 3*B*) as well as the absence of metabolic labeling of exogenous gangliosides with radioactive donor substrates shown in supplemental Fig. S1 preclude the possibility that exogenous GM3 is used by the cells for intracellular GD3 synthesis.

Inhibition of Vesicular Membrane Mobilization by ATP Depletion Reduces GD3 Synthesis at the Cell Surface—The biochemical experiments demonstrate that ecto-Sial-T2 may use endogenously synthesized CMP-NeuAc for synthesis of GD3. To investigate this hypothesis further that no ecto-Sial-T2 internalization is required for GD3 synthesis at the cell surface, we attempted to inhibit intracellular vesicular transport by depletion of ATP (28–30) and analyzed GD3 synthesis at the cell surface under different experimental conditions in P4-treated CHO-K1$^{Sial\text{-}T2+}$ cells. As expected, ATP depletion severely inhibited Alexa Fluor 647-transferrin endocytosis and did not significantly modify the amount of Sial-T2 present at the cell surface (Fig. 4*A*). However, although a reduced synthesis of GD3 at the cell surface was observed in ATP-depleted cells incubated in a medium containing bivalent cations in the absence of exogenous CMP-NeuAc (Fig. 4*B*), the incubation of ATP-depleted cells with exogenous CMP-NeuAc significantly restored the synthesis of GD3 to an intermediate level similar to that observed under control conditions (Fig. 4*B*). Taken together, these results suggest that GD3 synthesis at the cell surface depends on endogenously synthesized CMP-NeuAc, which probably arrives at the extracellular milieu by using the secretory pathway. Moreover, results also reinforce the hypothesis that GD3 synthesis occurs at the cell surface

through an enzymatic mechanism that is independent of Sial-T2 internalization.

Cell Surface GD3 Synthesis in SK-Mel-28 Human Melanoma Cells—Next, we examined ecto-Sial-T2 activity in SK-Mel-28 human melanoma cells which endogenously synthesize sialyltransferase and express ganglioside GD3 (Fig. 5) (13, 31). Sial-T2 activity on the SK-Mel-28 cell surface was measured following essentially the same protocol described above for CHO-K1$^{\text{Sial-T2+}}$ cells. As observed in Fig. 5, P4 treatment significantly reduced GD3 expression at the cell surface of SK-Mel-28 cells. However, if P4-treated SK-Mel-28 cells were fed with exogenous GM3 (Sial-T2 substrate) and incubated at 37 °C in a medium containing bivalent cations in the absence of exogenous CMP-NeuAc, an appreciable synthesis of GD3 was observed (Fig. 5, *third row*). As already observed for CHO-K1$^{\text{Sial-T2+}}$ cells, the addition of exogenous CMP-NeuAc further increased the synthesis of disialoganglioside (Fig. 5, *bottom row*).

Ecto-Sial-T2 activity in SK-Mel-28 cells was also investigated by flow cytometric analysis (Fig. 5, *right panels*). The Sial-T2 activity values at the cell surface of SK-Mel-28 cells, as measured by mean fluorescent intensity, were low in P4-treated cells. However, a noticeable increase in the mean fluorescent intensity was observed for the other analyzed experimental conditions (GM3 plus cations, and GM3 plus cations and exogenous CMP-NeuAc) in agreement with results obtained by confocal immunofluorescent analysis (Fig. 5, *left panels*). As already observed for CHO-K1$^{\text{Sial-T2+}}$ cells, the inhibition of vesicular membrane mobilization by ATP depletion also significantly reduced GD3 synthesis at the cell surface of SK-Mel-28 (supplemental Fig. S2). Thus, these results reveal cell surface GD3 synthesis in SK-Mel-28 human melanoma cells endogenously expressing Sial-T2, which minimizes the possibility that the ecto-Sial-T2 activity observed in

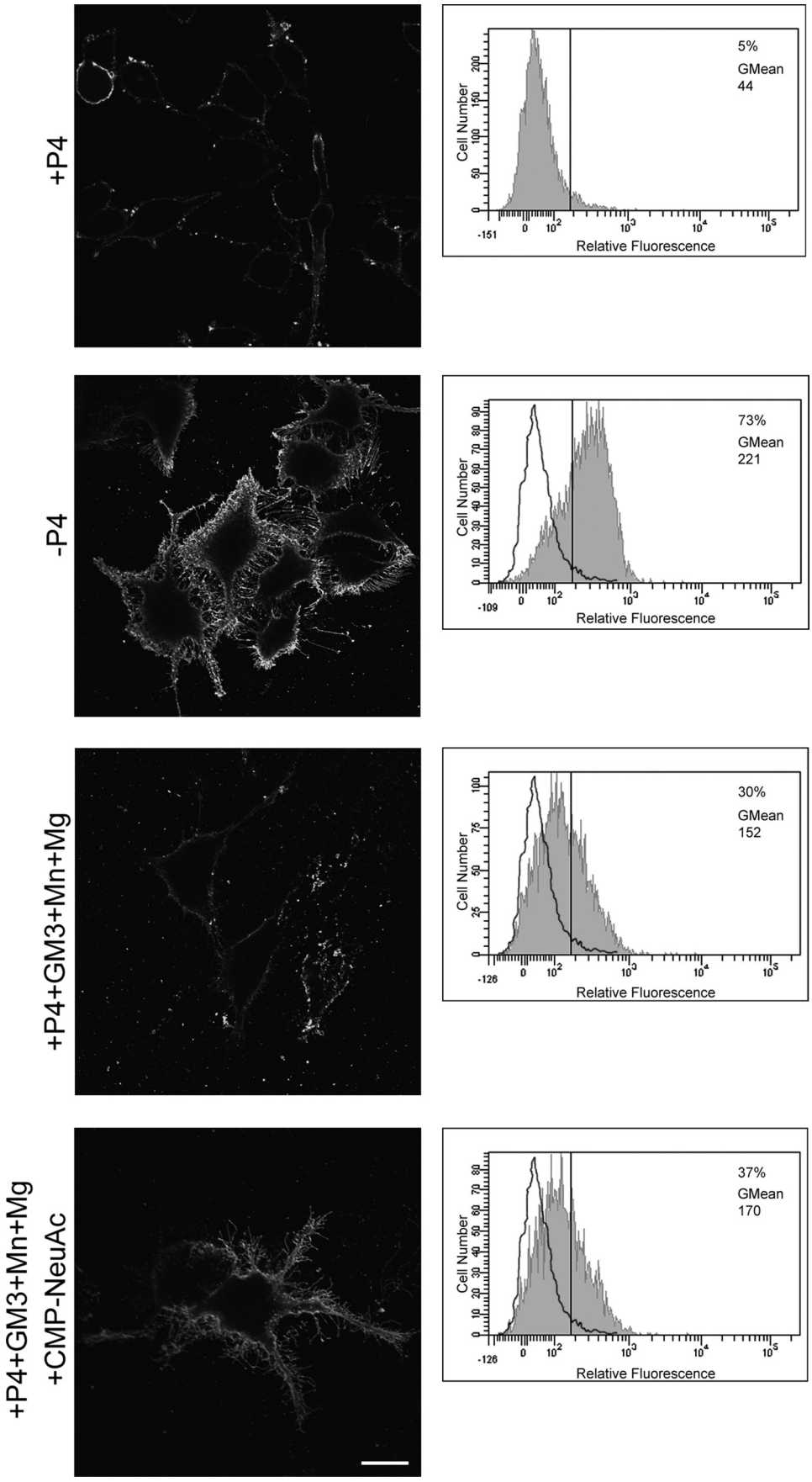

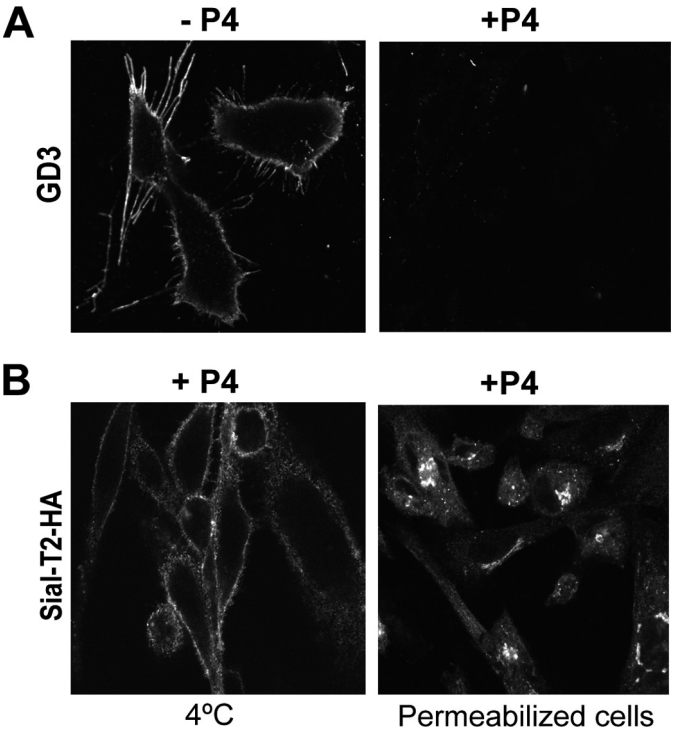

FIGURE 6. **Cell surface expression of Sial-T2 in glycolipid-depleted CHO-K1 cells.** *A*, CHO-K1$^{Sial\text{-}T2+}$ cells were grown on coverslips for 4 days in DMEM (−*P4*) or in DMEM containing P4 (+*P4*) to reduce the content of glycolipids. Then, cells were fixed and labeled for GD3 using the R24 antibody. *B*, CHO-K1$^{Sial\text{-}T2+}$ cells were grown on coverslips for 4 days in DMEM containing P4. Then, Sial-T2-HA-expressing cells were immunostained with antibody to HA at 4 °C for 60 min and then fixed and incubated with a secondary antibody conjugated to Alexa Fluor 488 (4 °C, *left panel*). Alternatively, cells were fixed and permeabilized before immunostaining of HA epitope (*Permeabilized cells*, *right panel*). Single confocal sections were taken every 0.7 μm parallel to the coverslip.

CHO-K1$^{Sial\text{-}T2+}$ cells was a consequence of the overexpression of the recombinant construct.

Expression of Sial-T2 at the Cell Surface Does Not Depend on the Synthesis of Glycolipid Substrates or Products—We next attempted to evaluate the role of glycolipids, including the substrate and product of Sial-T2, on the cell surface localization of the enzyme. To obtain cells with a reduced content of all glycosphingolipid classes, CHO-K1$^{Sial\text{-}T2+}$ cells were treated with P4, an inhibitor of ceramide glucosyltransferase and hence of the synthesis of GlcCer and of more complex glycolipids (25, 32). Exposure of cells to 2 μM P4 in the culture medium for 4 days led to a dramatic decrease of GD3 content with respect to control cells (Fig. 6*A*, see +*P4*). Under these experimental conditions, Sial-T2 was even observed at the cell surface and in the Golgi complex (Fig. 6*B*), discarding the possibility that transport of Sial-T2 to the plasma membrane could be associated with synthesis and vesicular exocytic transport of glycolipids.

Luminal Catalytic Domain of Sial-T2 Is Necessary for Its Localization at the Cell Surface—Sial-T2 is a type II membrane protein, consisting of a short cytosolic tail, a transmembrane region, and a luminally oriented catalytic domain (33). To evaluate the impact of catalytic domain deletion on the presence of Sial-T2 at the cell surface, CHO-K1^{WT} cells were transiently or stably transfected with a plasmid coding for the N terminus of Sial-T2 (amino acids 1–57 containing the cytosolic and transmembrane region) fused to the N terminus of YFP (Sial-T2-NTD-YFP) (Fig. 7*A*). The expression of the fluorescent construct both in live cells at 4 °C and in permeabilized cells was evaluated by analyzing the intrinsic fluorescence of YFP and by double immunofluorescence using an antibody to GFP, respectively. As shown in Fig. 7*B*, transiently or stably expressed Sial-T2-NTD-YFP was localized mainly at the Golgi complex but not at the cell surface for all tested experimental conditions (4 °C and permeabilized cells). Thus, these results strongly suggest that the luminal domain of Sial-T2, but not the catalytic activity on glycolipid substrates (see results from Fig. 6), is involved in its sorting and/or retention at the cell surface and rules out a mislocalization of the enzyme by overexpression.

N-Glycan Processing Status of Cell Surface-located Sial-T2—Chick Sial-T2 contains three conserved *N*-glycosylation sites (Asn-57, -105, and -200). In previous works, we demonstrated in CHO-K1 cells that most of the Golgi-located chick Sial-T2 was in an Endo-H-sensitive NANase-insensitive form. However, a minor secreted form lacking about 40 amino acids from the N terminus was Endo-H-resistant and NANase-sensitive, indicating that the cells were able to process *N*-glycans to an Endo-H-resistant form (23, 34). Bearing in mind these antecedents and by analyzing the *N*-glycan status, we decided to explore whether the plasma membrane-associated Sial-T2 partially or totally contributes to the soluble extracellular fraction of the enzyme. Cells were incubated at 4 °C with an antibody to HA and ecto-Sial-T2 immunoprecipitated (plasma membrane fraction). By using a second cycle of immunoprecipitation, Sial-T2 from the remnant homogenate was also recovered (intracellular fraction). As shown in Fig. 8, both these Sial-T2 fractions were Endo-H-sensitive and NANase-insensitive, strongly suggesting that the secreted form of Sial-T2 (Endo-H-resistant and NANase-sensitive) did not come from the cell surface fraction and consequently, that terminal glycosylation (sialylation and incorporation of the *N*-acetylglucosamines) and processing of *N*-glycans of Sial-T2 are not essential for its proper sorting and localization at the cell surface. In addition, quantitative analysis of Western blots (normalized for loading

FIGURE 5. **GD3 synthesis at the cell surface of SK-Mel-28 human cells endogenously expressing Sial-T2.** SK-Mel-28 cells were grown with P4 (+*P4*; *first*, *third*, and *fourth rows*) or without P4 (−*P4*, *second row*) for 4 days. Then, cells were treated with 100 μM GM3, washed, and incubated at 37 °C for 2 h in a medium containing Mn^{2+} and Mg^{2+} (+*P4*+*GM3*+*Mn*+*Mg*, *third row*), or CMP-NeuAc, Mn^{2+} and Mg^{2+} (+*P4*+*GM3*+*Mn*+*Mg*+*CMP*−*NeuAc*, *fourth row*). P4 inhibitor remained present throughout the experiments. *Left panels*, cells were washed, immunostained with antibody to GD3 (R24) at 4 °C for 1 h and then fixed and incubated with secondary antibody conjugated to Alexa Fluor 488. Single confocal sections were taken every 0.7 μm parallel to the coverslip. *Right panels*, cells were trypsinized, incubated at 4 °C with R24 antibody for 30 min, and then fixed and exposed to the secondary antibody for 30 min at 4 °C. Labeled cells were washed and resuspended in 200 μl of PBS, and fluorescence was quantified using flow cytometric analysis. The *vertical line* in each histogram marks the upper limit of control (+P4) to assess frequencies (%) of positive cells. The geometric mean fluorescence intensity (*GMean*) is also indicated. *Scale bar*, 10 μm.

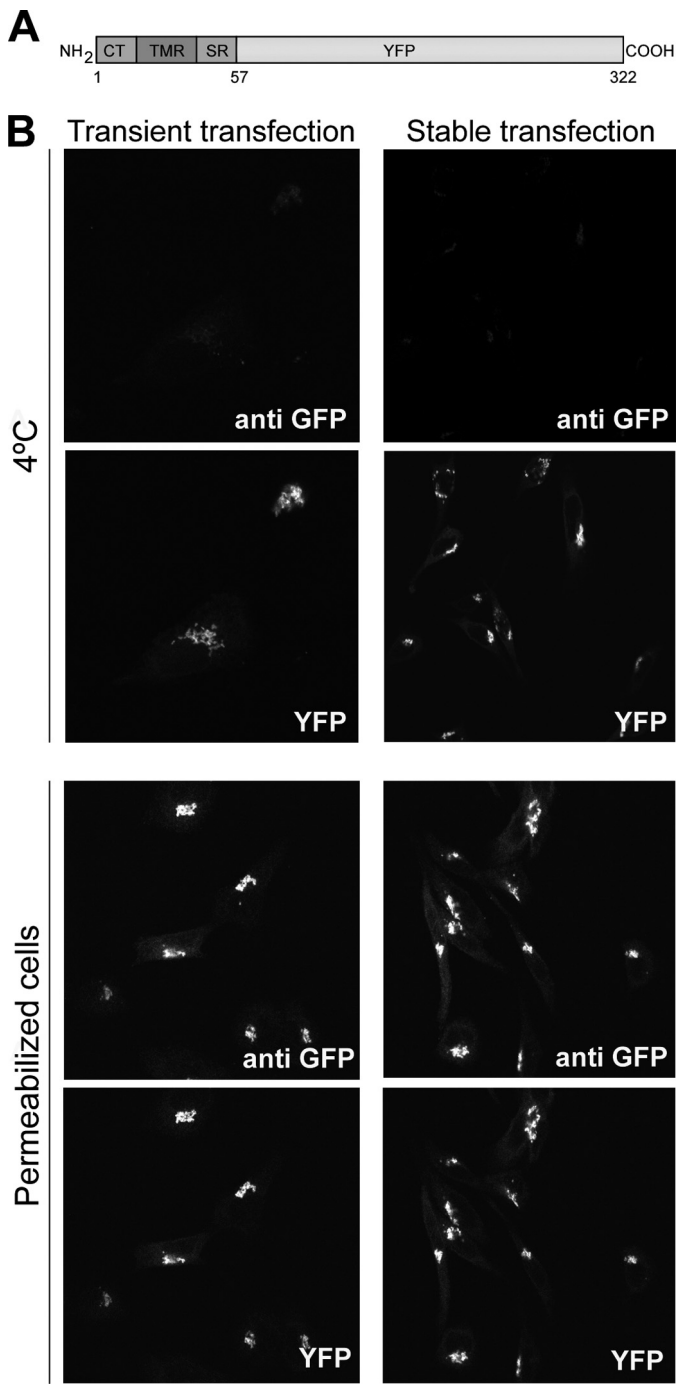

FIGURE 7. **The catalytic domain of Sial-T2 is necessary for its localization at the plasma membrane of CHO-K1 cells.** *A*, schematic representation of the Sial-T2-NTD-YFP construct is shown. *CT*, cytoplasmic tail; *TMR*, transmembrane region; *SR*, stem region; *YFP*, yellow fluorescence protein. *B*, CHO-K1^{WT} cells were transiently (*left panels*) or stably (*right panels*) transfected with the Sial-T2-NTD-YFP construct. Cells were immunostained with an antibody to GFP (*anti GFP*) at 4 °C for 60 min and then fixed and incubated with a secondary antibody conjugated to Alexa Fluor 488 (*4 °C, first row*); or cells were fixed, permeabilized, and immunostained with the antibody to GFP (*Permeabilized cells*, *third row*). The expression of the fluorescent construct was also evaluated by analyzing under each experimental condition the intrinsic fluorescence of YFP (*second* and *fourth rows*). Single confocal sections were taken every 0.7 μm parallel to the coverslip.

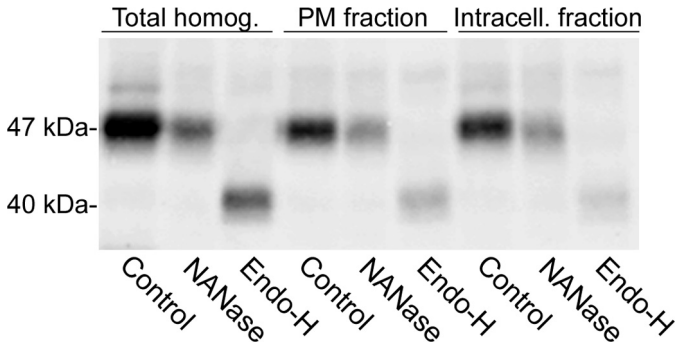

FIGURE 8. ***N*-Glycosylation status of plasma membrane-associated Sial-T2 in CHO-K1$^{Sial\text{-}T2+}$ cells.** Intact CHO-K1$^{Sial\text{-}T2+}$ cells in suspension were incubated at 4 °C with antibody to HA for 45 min. After washing, cells were lysed, and the Sial-T2-HA·antibody complex was recovered using protein A-Sepharose beads (*PM fraction*). The supernatant, containing the intracellular fraction of Sial-T2-HA, was subjected to a second cycle of immunoprecipitation with antibody to HA and protein A-Sepharose beads (*Intracell. fraction*). Additionally, total Sial-T2-HA was also recovered from homogenates of CHO-K1$^{Sial\text{-}T2+}$ cells (*Total homog.*). Fractions from immunoprecipitates were incubated in PBS (*Control*) or in a medium containing NANase or Endo-H. After incubation, samples were Western blotted with antibody to HA. The positions and sizes of the different Sial-T2 forms are indicated on the *left*.

variations) allowed us to estimate the amount of Sial-T2 present at the cell surface of the CHO-K1$^{Sial\text{-}T2+}$ cells at 11% (supplemental Fig. S3*A*). This percentage was slightly lower (5.2%) when the amount of ecto-Sial-T2 was evaluated by cell surface biotinylation using the membrane-impermeable EZ-link Sulfo-NHS-SS-Biotin reagent and precipitation by streptavidin-agarose beads (supplemental Fig. S3*B*).

GalNAc-T but Not Gal-T2 Is Also Expressed at the Cell Surface and Requires Exogenous Substrates to Exert Enzymatic Activity—The expression and activity of Sial-T2 was demonstrated on plasma membrane from CHO-K1 and SK-Mel-28 cells. On the other hand, results from the biochemical experiments shown in Fig. 2 did not reveal enzymatic activity of GalNAc-T or Gal-T2 on the cell surface of CHO-K1 cells. To explore further the expression and activities of these glycosyltransferases at the cell surface, CHO-K1 cells stably expressing both GalNAc-T-myc and Gal-T2-HA (clone 4) were processed as indicated in Fig. 1, with the expression of GalNAc-T-myc and Gal-T2-HA being revealed by confocal immunofluorescence microscopy. As shown in Fig. 9*A*, GalNAc-T-myc but not Gal-T2-HA was found decorating the cell surface of CHO-K1 cells, whereas in permeabilized cells both GalNAc-T-myc and Gal-T2-HA showed the typical perinuclear localization characteristic of the Golgi complex. As control, we observed that CHO-K1^{WT} did not bind the antibody to HA or c-Myc. Taking these results into consideration, we hypothesize that the lack of enzymatic activity observed for GalNAc-T on the plasma membrane of CHO-K1 cells (see Fig. 2) was a consequence of the reduced levels of acceptor substrate (GM3) expressed in clone 4 (26). To test this assumption, cells from clone 4 were fed with 100 μM GM3 and then with UDP-[^{3}H]GalNAc to label GM2. Although the chromatographic analysis of purified glycolipids revealed a synthesis of GM2, this was not observed when GM3 substrate was omitted (−*GM3*, Fig. 9*B*). To investigate further the Gal-T2 activity and coupling of glycosyl transfer steps (35) in the synthesis of GM1 at the plasma membrane, cells from clone 4 were fed with GM3 and then incubated with UDP-[^{3}H]GalNAc and UDP-[^{3}H]Gal (necessary for the transfer step that would use

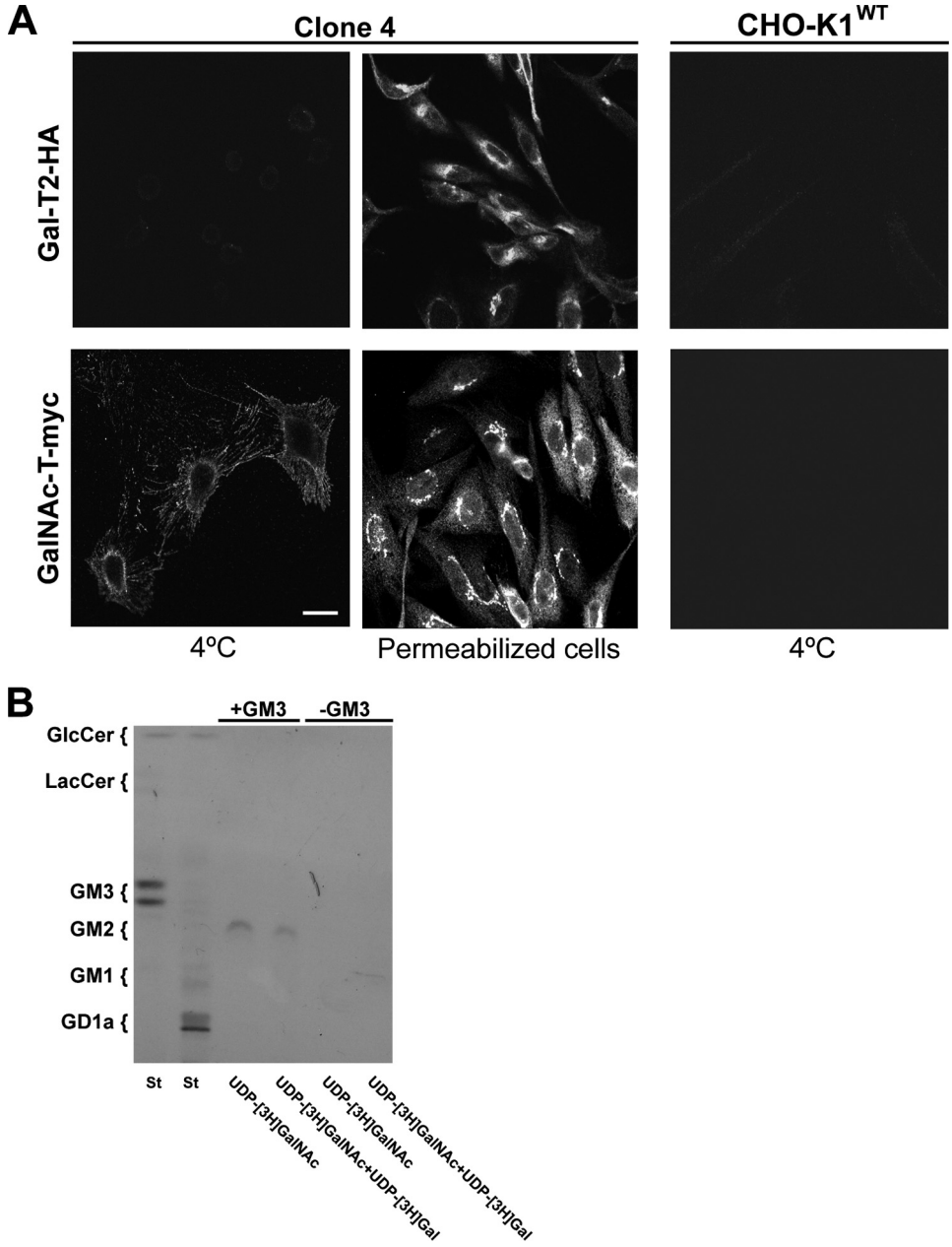

FIGURE 9. **Immunofluorescence detection and activity of GalNAc-T and Gal-T2 at the cell surface of CHO-K1 cells.** *A*, wild-type CHO-K1 cells (CHO-K1^{WT}) or CHO-K1 cells stably expressing both GalNAc-T-myc and Gal-T2-HA (clone 4) were immunostained with antibody to HA (*first row*) at 4 °C for 60 min and then fixed and incubated with secondary antibody conjugated to Alexa Fluor 488 (*4* °C). Alternatively, cells from clone 4 were fixed and permeabilized before immunostaining with antibody to HA (*Permeabilized cells*). In another set of experiments, CHO-K1^{WT} cells or CHO-K1 cells stably expressing both GalNAc-T-myc and Gal-T2-HA (*Clone 4*) were immunostained with antibody to c-Myc (*second row*) at 4 °C for 60 min and then fixed and incubated with secondary antibody conjugated to Alexa Fluor 488 (4 °C). In addition, cells from clone 4 were fixed and permeabilized before immunostaining with antibody to c-Myc (*Permeabilized cells*). The image contrast in CHO-K1^{WT} cells was reduced to show the presence of cells. *Scale bar*, 10 μm. *B*, cells from clone 4 previously treated (+*GM3*) or not (−*GM3*) with 100 μM GM3 were incubated with UDP-[^{3}H]GalNAc or UDP-[^{3}H]GalNAc and UDP-[^{3}H]Gal for 2 h. Next, lipid extracts were purified, chromatographed, and visualized as indicated under "Experimental Procedures." The positions of the co-chromatographed radioactive glycolipid standards (*St*) are indicated on the *left* of the *plate*.

the radioactive GM2 formed in the first step). Under this experimental condition, we observed that radioactive GM2 did not progress to GM1, thus further supporting the absence of Gal-T2 activity on the cell surface.

In conclusion, these results reveal that GalNAc-T but not Gal-T2 is expressed on CHO-K1 cell surface. In addition, catalytic transference of GalNAc to GM3 was observed when cells were fed with acceptor glycolipid substrate.

DISCUSSION

We have explored in this work the expression and activity of ganglioside glycosyltransferases at the cell surface of epithelial and melanoma cells. Both ectopically and endogenously expressed Sial-T2 were found to be able to sialylate GM3 at the plasma membrane using both the exogenous and endogenous donor (CMP-NeuAc) and the acceptor (GM3) substrates. Furthermore, using an optimized intact cell labeling approach, we did not detect Sial-T1, Sial-T4, Gal-T2, or GalNAc-T enzyme activities at the cell surface of CHO-K1 cells. However, expression of GalNAc-T was observed, whose catalytic activity was only evidenced after feeding the cell with exogenous GM3 substrate.

It was also demonstrated that the expression of ecto-Sial-T2 was not associated with the synthesis and vesicular exocytic transport of glycolipids and moreover, was independent of its catalytic activity. Nevertheless, it was found that the luminal domain of Sial-T2 was necessary for its sorting and/or retention at the cell surface. Related to this, it has been already shown that Sial-T2 mostly localizes at the proximal Golgi and contains three *N*-glycosylation sites occupied by *N*-glycans (23, 34). Consistent with its sub-Golgi location, most of the enzyme was found to exist in an Endo-H-sensitive NANase-insensitive form, whereas some occurred as a secreted Endo-H-resistant and NANase-sensitive form lacking ~40 amino acids (23). Analysis of the *N*-glycan processing status of ecto-Sial-T2 (Endo-H-sensitive, NANase-insensitive) discarded the possibility that the released form of Sial-T2 resulted from a proteolytic cleavage of ecto-Sial-T2. In addition, it is known that glycoproteins moving along the secretory pathway and progressing beyond the medial Golgi suffer the successive action of the processing enzymes *N*-acetylglucosaminyltransferase 1 and mannosidase II, thereby acquiring Endo-H resistance and terminal

glycosylation (*i.e.* sialylation) of their *N*-glycans (36). Thus, the *N*-glycan status of ecto-Sial-T2 strongly suggests that it might arrive at the plasma membrane from the medial Golgi through using a secretory trans-Golgi network bypass route or directly by a Golgi-independent trafficking, as previously suggested for both polarized and nonpolarized cells (37, 38).

It is known that CMP-NeuAc is synthesized at the nucleus (39, 40). Then, it diffuses into the cytoplasm, where it is specifically transported into the lumen of the Golgi complex by the CMP-NeuAc antiporter which facilitates both the influx of the nucleotide-activated sugar and the efflux of CMP out the Golgi complex (41). The CMP-NeuAc transporter is located in the medial-trans cisternae of the Golgi complex but not in the other extra-Golgi compartments, including the plasma membrane (41). This implies that luminal nucleotide sugar diffuses freely throughout the Golgi complex until encountering sialyltransferases, which are found in different Golgi cisternae. According to the results shown in this work, we hypothesize that CMP-NeuAc might also use the secretory via to arrive at the extracellular milieu, where it is then used by the plasma membrane-associated Sial-T2 to synthesis GD3. Supporting this assumption, the presence of CMP-NeuAc in human serum has been previously demonstrated (42–44).

The possibility was also considered that ecto-Sial-T2 could be catalyzing the synthesis of GD3 during an endocytic process in which GM3 is sialylated by ecto-Sial-T2 using intracellular CMP-NeuAc and then being redirected to the plasma membrane. However, we discarded this hypothesis because it was observed that ecto-Sial-T2-HA did not appreciably internalize and/or recycle over a period of 2 h when analyzed by an antibody-binding technique (results not shown). In addition, we also demonstrated that the impairment of plasma membrane internalization by treatment with impermeable fixative tannic acids (45, 46) did not affect synthesis of GD3 at the cell surface of CHO-K1$^{\text{Sial-T2+}}$ cells, although transferrin endocytosis was severely affected (results not shown).

The existence of ganglioside sialylation was previously reported in synaptosomal membrane from calf and rat brains and during the development of neuronal cell cultures (47–49). However, there was concern that cross-contamination of biochemically isolated membrane fractions may have occurred, and progress in this research area is still limited. More recently, the possible involvement of plasma membrane-associated Sial-T1 in GM3 synthesis in the thymuses of dexamethasone-administered mice has been suggested (50).

The cloning of genes for most of the glycosyltransferases responsible for ganglioside biosynthesis, together with the development of cell lines with modified glycolipid expression and new biochemical approaches, has allowed us to investigate in detail the expression and activity of ganglioside glycosyltransferases at the cell surface. The current scenario shows the presence of both ganglioside glycosyltransferases and glycohydrolases at the plasma membrane (*i.e.* Sial-T2 and Neu3 acting on the common substrate GM3), which may locally and rapidly modulate cellular glycolipid compositions in response to different external and internal stimuli. Additionally, ecto-Sial-T2 may have a physiologic role as an adhesion molecule in cell-cell or cell-extracellular matrix interaction, as has been shown for the surface-associated β1,4-galactosyltransferase (51, 52) and fucosyltransferase (53).

Acknowledgments—We thank C. Sampedro, G. Schachner, and S. Deza for technical assistance; G. Nores (CIQUIBIC, Córdoba, Argentina) for excellent assistance with GM3 purification from dog erythrocytes; and R. Iglesias-Bartolome (NIDCR, National Institutes of Health) for comments and discussions.

REFERENCES

1. Daniotti, J. L., Crespo, P. M., and Yamashita, T. (2006) *J. Cell. Biochem.* **99,** 1442–1451
2. Hakomori, S., Handa, K., Iwabuchi, K., Yamamura, S., and Prinetti, A. (1998) *Glycobiology* **8,** xi–xix
3. Miljan, E. A., and Bremer, E. G. (2002) *Sci. STKE* 2002, re15
4. Proia, R. L. (2003) *Philos. Trans R. Soc. Lond. B Biol. Sci.* **358,** 879–883
5. Zurita, A. R., Crespo, P. M., Koritschoner, N. P., and Daniotti, J. L. (2004) *Eur. J. Biochem.* **271,** 2428–2437
6. Zurita, A. R., Maccioni, H. J., and Daniotti, J. L. (2001) *Biochem. J.* **355,** 465–472
7. Maccioni, H. J., Daniotti, J. L., and Martina, J. A. (1999) *Biochim. Biophys. Acta* **1437,** 101–118
8. Tettamanti, G. (2004) *Glycoconj. J.* **20,** 301–317
9. Crespo, P. M., Iglesias-Bartolomé, R., and Daniotti, J. L. (2004) *J. Biol. Chem.* **279,** 47610–47618
10. De Matteis, M. A., and Luini, A. (2008) *Nat. Rev. Mol. Cell Biol.* **9,** 273–284
11. van Meer, G., and Holthuis, J. C. (2000) *Biochim. Biophys. Acta* **1486,** 145–170
12. van Meer, G., and Lisman, Q. (2002) *J. Biol. Chem.* **277,** 25855–25858
13. Iglesias-Bartolomé, R., Crespo, P. M., Gomez, G. A., and Daniotti, J. L. (2006) *FEBS J.* **273,** 1744–1758
14. Iglesias-Bartolomé, R., Trenchi, A., Comín, R., Moyano, A. L., Nores, G. A., and Daniotti, J. L. (2009) *Biochim. Biophys. Acta* **1788,** 2526–2540
15. Mayor, S., and Pagano, R. E. (2007) *Nat. Rev. Mol. Cell Biol.* **8,** 603–612
16. Yu, R. K., Bieberich, E., Xia, T., and Zeng, G. (2004) *J. Lipid Res.* **45,** 783–793
17. Kopitz, J., von Reitzenstein, C., Mühl, C., and Cantz, M. (1994) *Biochem. Biophys. Res. Commun.* **199,** 1188–1193
18. Papini, N., Anastasia, L., Tringali, C., Croci, G., Bresciani, R., Yamaguchi, K., Miyagi, T., Preti, A., Prinetti, A., Prioni, S., Sonnino, S., Tettamanti, G., Venerando, B., and Monti, E. (2004) *J. Biol. Chem.* **279,** 16989–16995
19. Valaperta, R., Chigorno, V., Basso, L., Prinetti, A., Bresciani, R., Preti, A., Miyagi, T., and Sonnino, S. (2006) *FASEB J.* **20,** 1227–1229
20. Mencarelli, S., Cavalieri, C., Magini, A., Tancini, B., Basso, L., Lemansky, P., Hasilik, A., Li, Y. T., Chigorno, V., Orlacchio, A., Emiliani, C., and Sonnino, S. (2005) *FEBS Lett.* **579,** 5501–5506
21. Aureli, M., Masilamani, A. P., Illuzzi, G., Loberto, N., Scandroglio, F., Prinetti, A., Chigorno, V., and Sonnino, S. (2009) *FEBS Lett.* **583,** 2469–2473
22. Prinetti, A., Chigorno, V., Mauri, L., Loberto, N., and Sonnino, S. (2007) *J. Neurochem.* **103,** 113–125
23. Daniotti, J. L., Martina, J. A., Giraudo, C. G., Zurita, A. R., and Maccioni, H. J. (2000) *J. Neurochem.* **74,** 1711–1720
24. Giraudo, C. G., Rosales Fritz, V. M., and Maccioni, H. J. (1999) *Biochem. J.* **342,** 633–640
25. Crespo, P. M., Zurita, A. R., and Daniotti, J. L. (2002) *J. Biol. Chem.* **277,** 44731–44739
26. Crespo, P. M., Zurita, A. R., Giraudo, C. G., Maccioni, H. J., and Daniotti, J. L. (2004) *Biochem. J.* **377,** 561–568
27. Martin, O. C., and Pagano, R. E. (1987) *J. Biol. Chem.* **262,** 5890–5898
28. Podbilewicz, B., and Mellman, I. (1990) *EMBO J.* **9,** 3477–3487
29. Smalley, K. S., Koenig, J. A., Feniuk, W., and Humphrey, P. P. (2001) *Br. J. Pharmacol.* **132,** 1102–1110
30. Troyanovsky, R. B., Sokolov, E. P., and Troyanovsky, S. M. (2006) *Mol. Biol. Cell* **17,** 3484–3493

31. Pukel, C. S., Lloyd, K. O., Travassos, L. R., Dippold, W. G., Oettgen, H. F., and Old, L. J. (1982) *J. Exp. Med.* **155,** 1133–1147
32. Li, R., Manela, J., Kong, Y., and Ladisch, S. (2000) *J. Biol. Chem.* **275,** 34213–34223
33. Colley, K. J. (1997) *Glycobiology* **7,** 1–13
34. Martina, J. A., Daniotti, J. L., and Maccioni, H. J. (1998) *J. Biol. Chem.* **273,** 3725–3731
35. Giraudo, C. G., Daniotti, J. L., and Maccioni, H. J. (2001) *Proc. Natl. Acad. Sci. U.S.A.* **98,** 1625–1630
36. Kornfeld, R., and Kornfeld, S. (1985) *Annu. Rev. Biochem.* **54,** 631–664
37. Saraste, J., Dale, H. A., Bazzocco, S., and Marie, M. (2009) *FEBS Lett.* **583,** 3804–3810
38. Tveit, H., Akslen, L. K., Fagereng, G. L., Tranulis, M. A., and Prydz, K. (2009) *Traffic* **10,** 1685–1695
39. Coates, S. W., Gurney, T., Jr., Sommers, L. W., Yeh, M., and Hirschberg, C. B. (1980) *J. Biol. Chem.* **255,** 9225–9229
40. Kean, E. L., Münster-Kühnel, A. K., and Gerardy-Schahn, R. (2004) *Biochim. Biophys. Acta* **1673,** 56–65
41. Zhao, W., Chen, T. L., Vertel, B. M., and Colley, K. J. (2006) *J. Biol. Chem.* **281,** 31106–31118
42. Gross, H. J., Merling, A., Moldenhauer, G., and Schwartz-Albiez, R. (1996) *Blood* **87,** 5113–5126
43. Parsons, N. J., Ashton, P. R., Constantinidou, C., Cole, J. A., and Smith, H. (1993) *Microb. Pathog.* **14,** 329–335
44. Smith, H., Parsons, N. J., and Cole, J. A. (1995) *Microb. Pathog.* **19,** 365–377
45. Paladino, S., Pocard, T., Catino, M. A., and Zurzolo, C. (2006) *J. Cell Biol.* **172,** 1023–1034
46. Polishchuk, R., Di Pentima, A., and Lippincott-Schwartz, J. (2004) *Nat. Cell Biol.* **6,** 297–307
47. Durrie, R., Saito, M., and Rosenberg, A. (1988) *Biochemistry* **27,** 3759–3764
48. Matsui, Y., Lombard, D., Massarelli, R., Mandel, P., and Dreyfus, H. (1986) *J. Neurochem.* **46,** 144–150
49. Preti, A., Fiorilli, A., Lombardo, A., Caimi, L., and Tettamanti, G. (1980) *J. Neurochem.* **35,** 281–296
50. Iwamori, M., and Iwamori, Y. (2005) *Glycoconj. J.* **22,** 119–126
51. Begovac, P. C., Shi, Y. X., Mansfield, D., and Shur, B. D. (1994) *J. Biol. Chem.* **269,** 31793–31799
52. Miller, D. J., Macek, M. B., and Shur, B. D. (1992) *Nature* **357,** 589–593
53. Raychoudhury, S. S., and Millette, C. F. (1997) *Biol. Reprod.* **56,** 1268–1273